

# New Multi-Stage Centrifugal Turbines for Power Plant Driven By Solar Energy

Ayad M. Salman

Energy and Renewable Energies Technology Center, University of Technology, Baghdad-Iraq  
Email: 11017 @ uotechnology.edu.iq

**Abstract**— Due to continuously increasing oil prices, global warming concern and depletion of fossil fuels need to be considered as vital issues and requires direct exploration for alternative sources of energy. Therefore, organic Rankine cycle can be probably considered as one of the most flexible technologies in terms of power level capacity and the required heat source temperature. This study explores the performance of unconventional two-stage expander type of radial-outflow turbine for organic Rankine power system where the expander is considered as the heart of the power system. The main aim of the current work is to present new study based on the computational fluid dynamic using ANSYS-CFX to evaluate the performance of a small-scale two-stage expander for ORC system and fluid dynamic characterization of the flow through the flow passages inside the expander stage. The simulations results showed that the expander isentropic efficiency was around 76.1% which is slightly less than 1.5% delivered from mean-line design using zTurbo. While, the maximum deviation with the obtained efficiency from mean-line design based on thermodynamic analysis at mid-span was 2.2% compared with computational fluid dynamic simulations results. This deviation is due to the tip leakage and complexity of flow that it can't be captured by one-dimensional analysis.

**Keywords**— Power plant, multi-stage, solar energy.

## I. INTRODUCTION

Recently, global economies and energy demands have been struggling to search a suitable energy sources needed further technology investigation and development. Renewable energy sources are available and can be driven the power system for small and large power capacity. Moreover, the power in small to medium applications is play a key role in future energy market. Therefore, the conversion of waste heat energy and renewable energy are highly demand.

The mean-line design of the radial outflow expander for organic Rankine cycle was considered in [1]. Two organic fluids (Siloxane namely MDM) were used with mass flow rate of 22 kg/s and rotational speed of 3000 rpm. The output from the mean-line design showed that the expander efficiency and power were 87.86% and 1.2 MW respectively. Mean-line design and computational fluid dynamics simulations for 1 MW organic Rankine cycle (ORC) based on radial outflow expander were reported in [2]. Mean-line design for 10 kW ORC radial outflow driven by waste thermal energy was conducted in [3]. Mean-line design was carried out based Craig-Cox loss model in order to predict the loss across the flow passages of the radial outflow expander. Small scale axial, radial inflow and outflow expanders for organic Rankine system applications has been investigated in [4-6] for various working fluids and low mass flow rate ranged between 0.1 to

0.5 kg/s. The analysis was conducted based on mean-line design and CFD analysis technique. The small-scale expanders performance indicated that the maximum efficiency around 84% and power around 15 kW were achieved.

The real-gas flow as organic fluid flows over expander cascade blade/airfoil has been investigated in [7]. Where, the simulations of turbulent viscous flow of the real-gas working fluid through the nozzle of radial expander were carried out. Moreover, numerical simulation to investigate the effect of the real-gas flow of the high density working fluid over radial cascade expander was carried out in [8]. Radial inflow expander was designed for organic Rankine system and tested experimentally in [9]. Where, R123 as organic fluid was used with expander inlet temperature of 100°C. The maximum expander efficiency of 68% was obtained. In ORC systems, the small stages number leads high expansion ratios and transonic and supersonic expanders. Moreover, the shock waves in highly dissipative components are normally initiate in expanders when the components operate at part load as reported in [10, 11].

Mini organic Rankine system was examined and developed the small power expander as reported in [12] depending on applications of low-temperature thermal sources and various working fluids in order to costume the expander design requirements. Finally, the possibly vast change of range power and implemented operating conditions, working fluids and thermo-dynamic analysis were investigated. Where, radial outflow expander is down-scaling up to 10 kW for mini organic Rankine cycle architecture for various organic fluids.

The similitude theory was applied to investigate the performance of both radial inflow expander and organic Rankine system based on dynamics model, off-design and steady-state conditions as reported [13]. Axial expander in small scale configuration was investigated experimentally using R245fa and HFE7100 as the working fluids as reported in [14]. The maximum efficiency and power were 59.7% and 1.979 kW respectively. The possible of using solar energy to run the power plant as reported in [15].

Mean-line design model for radial inflow expander was built for organic Rankine cycle powered by geothermal energy as detailed in [16]. In mean-line design, the heat losses model was applied and the CFX software was used in order to 3D CFD simulations. Moreover, the optimization genetic algorithm was employed to optimize the expander. Two stage axial models was developed and investigated analytically to predict the relationship between equivalent area ratio and the expander load split under steady-state condition which

presented in [17]. Where, the load split between the low pressure expander (LPE) and HIGH Pressure expander (HPE) was verified based on experimental data which was revealed by the model.

To the author’s knowledge, the modelling of small scale radial outflow expander for organic Rankine system is limited and still missing due to the available losses model of the expander which is available for large power system and air ideal gas as a working fluid. Due to the difference in the expander geometries and flow conditions, the precision of the existing loss model of the expander becomes questionable when applied in prediction of small scale expander performance. Therefore, the new current model can be used to predict the performance of small scale radial outflow expander due to combined the mean-line design, CFD simulations and organic Rankine cycle which delivered more accurate performance.

## II. MEAN-LINE DESIGN FOR RADIAL OUTFLOW EXPANDER

Figure (1) shows the simplified radial outflow expander stage [18]. Mean-line design of the radial outflow expander is complex due to absence of the experimental data about the organic expander in the open literature.

The mean-line design of radial outflow expander is derived from axial expander which may shows dissimilar velocity triangle per expander stage and unusual channel shape i.e. converge from first stage and diverge for others stages. The loading ( $\psi$ ) and flow ( $\phi$ ) coefficients with degree of reaction (R) were used as dimensionless parameter in order to investigate the performance and velocity triangle of the radial flow expander. The velocity triangle in terms of angle at expander stage inlet and exit can be obtained as following [19]:

$$\left. \begin{aligned} \tan \beta_2 &= \frac{(\psi - 2R)}{2\phi} \\ \tan \beta_3 &= \frac{-(\psi + 2R)}{2\phi} \\ \tan \alpha_3 &= \frac{-(\psi/2 - (1 - R))}{\phi} \\ \tan \alpha_2 &= \frac{(\psi/2 + (1 - R))}{\phi} \end{aligned} \right\} \quad (1)$$

The blade height and chord for radial outflow expander have an effect on the distribution of the blade lengthways the expander stage diameter. The section area and inner and outer diameter of the expander stage are calculated as following:

$$A_{out} = H_{out} o = \frac{\dot{m}}{\rho_{out} V_{out} N_{blids}} \quad (2)$$

$$D_{out} = D_{in} + b \quad (3)$$

where A, D and H are the stage cross section area, stage diameter and blade height respectively. P is the working fluid density. V and N are flow velocity and blade numbers.

The flow width (o) can be calculated as following:

$$o = S \cos(BDA) \quad (4)$$

where BDA is a blade discharge angle which is equivalent to outlet flow at nozzle and rotor exit.

The blade pitch (S) and blade height can be obtained based on the following equation:

$$S = \pi D_{out} / N_{blids} \quad (5)$$

$$H_{out} = \frac{\dot{m}}{\rho_{out} V_{out} \cos(BDA) D_{out} \pi} \quad (6)$$

The mean-line design of the radial outflow expander is established based on the AMDCKO (Ainley and Mathieson, Dunham and Cam, Kacker and Okapuu) losses model which includes the total pressure losses through the blade rows in terms of profile, trailing edge and secondary flow, and tip leakage losses. The total pressure losses through the blade passages can be formulated as following:

$$K_T = K_P f_{Re} + K_{Sec} + K_{TE} K_{TC} \quad (7)$$

where  $K_T$ ,  $K_P$ ,  $K_{Sec}$ ,  $K_{TE}$ ,  $K_{TC}$  represent total pressure losses and  $f_{Re}$  represent friction losses coefficient.

The expander isentropic efficiency in the expression of enthalpy losses as following:

$$\eta_{tt} = \frac{1}{1 + [\zeta_R W_3^2/2 + (\zeta_S C_2^2/2)(h_3/h_2)]/(h_{01} - h_{03})} \quad (8)$$

$$\eta_{ts} = \frac{1}{1 + [\zeta_R W_3^2/2 + (\zeta_S C_2^2/2)(h_3/h_2) + C_3^2/2]/(h_{01} - h_{03})} \quad (9)$$

where  $\eta_{tt}$  and  $\eta_{ts}$  are total-to-total and total-to-static isentropic efficiency.

The current work includes end-wall losses, counting the tip leakage, secondary, and trailing edge losses as detailed in [19].

The majority of the mean-line design for radial outflow is to provide the expander initial dimensions like: number of blades, chord length, blade pitch, trailing edge thickness and leading edge thickness. In the current research, the zTurbo was used to develop the mean-line design for radial outflow expander. The zTurbo code for mean-line design can investigate many configurations of radial outflow expander from where various input parameters namely: loading and flow coefficients, degree of reaction, hub to tip radius ratio, expander inlet pressure and temperature, rotational speed and mass flow rate.

## III. COMPUTATIONAL FLUID DYNAMIC SIMULATIONS MODEL

The three-dimensional geometry of the blade expander is created using ANSYS BladeGen module. Where, the expander stage consist from stator and rotor blades rows. The three-dimensional configuration for two-stage radial outflow expander is shown in Fig. 1. The initial expander dimensions from mean-line design in terms of number of baled, blade height and blade width, blade chord and trailing and leading edges thickness...etc. are exported to blade module to generate three-dimensional expander stage.

The three-dimensional blade configuration from BladeGen is exported to TurboGrid module in ANSYS workbench in order to meshing the flow passages as shown in Fig. 2. The meshing of the flow passages is based on hexahedral meshes mostly type of an O-H grid. Where, the implemented topology is generated using mesh type of H grid d with O grid type which is added at leading and trailing edges of the blade.

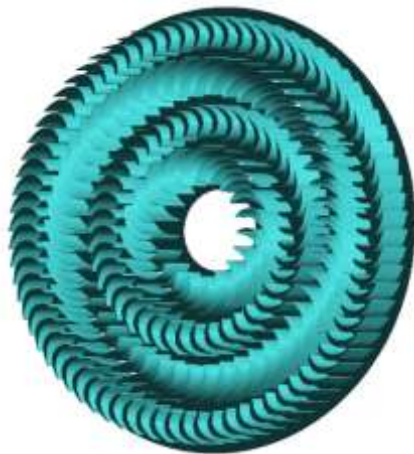


Fig. 1. Three dimensional view of the two stage expander.

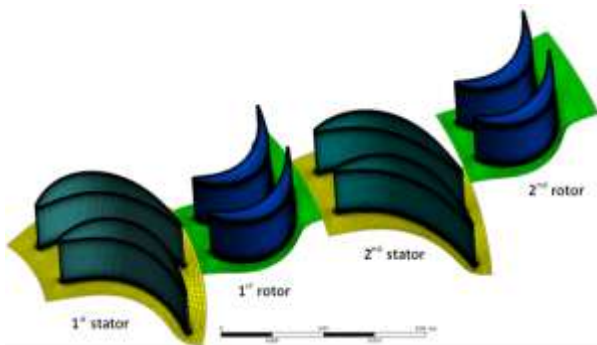


Fig. 2. Three-dimensional view of the grid generation of the flow passages.

Mesh independent study is carried out through the simulations processes in order to obtain the results independent on the number of meshes where expander isentropic efficiency and power are used as monitor parameters.

In CFD setup through CFX software, The Reynolds average Navier–Stokes (RANS) equations are solved together with k-omega/SST turbulence model to deliver accurate prediction of the expander stage performance and the flow characteristic through flow passages. R245fa was used as a working fluid in the current study based on Soave-Redlich-Kwong equation of state which is developed in terms of real gas equations and considered as one of the effective cubic equations model.

Obtaining a good communication between stator/rotor interfaces, the mixing-plane model was employed. The automatic wall function was applied in order to determine the viscosity effect near the wall due to the large gradient of dependent variables in terms of velocity components. The boundary conditions were set as: inlet total pressure and temperature with static pressure at outlet. The turbulence intensity was fixed at standard value of 5%. The flow was assumed subsonic at the expander stage inlet. The blade wall was treated as no slip, smooth and adiabatic conditions. Both Turbulence Numerics and Advection Scheme were set to High Resolution Scheme. The simulations convergence criterion was fixed at  $10^{-5}$  for all residual (RMS) values. The organic

fluid thermodynamic properties were gotten by REFPROP software.

#### IV. ORGANIC WORKING FLUIDS

One of the major challenges in organic Rankine system is selecting organic fluid. Therefore, it should be a balance between environmental concerns, commercial availability, thermodynamic performance and balance. R245fa as a working fluid was chosen based on above-mentioned criteria. Moreover, regarding to literature about selection organic working fluids, R245fa is considered one of the most suitable working fluids for low temperature heat sources.

The organic fluid has many influences on the expander size and other organic Rankine system components. Therefore, the choice of organic fluid is the fundamental step in organic Rankine system design.

#### V. RESULTS AND DISCUSSION

The aerodynamic flow characteristics and performance of two stage of radial outflow expander was designed, analyzed and simulated using three-dimensional computational fluid dynamics (CFD) based on ANSYS-CFX. For two stage expander configuration, the power output is about 15 kW with isentropic efficiency of 76.1% which is less than the predictable performance from the mean-line design at the design operating conditions. The operating conditions in terms of expander inlet temperature of 370 K, expansion ratio of 5.0 and rotational speed of 22000 rpm are investigate in the CFD simulations and mean-line design.

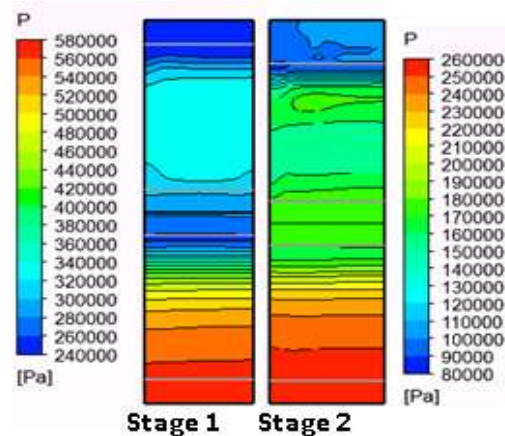


Fig. 3. Meridional pressure distribution through stage 1 and stage 2 of the radial outflow expander.

Fig. 3 shows the meridional pressure distribution through the expander stage 1 and stage 2 at design conditions. It can be seen that the maximum pressure was at expander inlet of the first stage and the minimum pressure was at the expander exit of the second stage. Fig. 4 displays the relative Mach number across the expander stages where the maximum relative Mach number was at rotor outlet of the second stage with value of 1.3. Fig. 5 illustrates temperature distribution achieved in the meridional plane of the expander stages. As can be seen, the maximum temperature of the working fluid at entrance of the expander first stage and the minimum temperature of 319 K

was noticed at the rotor exit of the second stage. The Mach number in terms of absolute flow velocity and relative flow velocity was showed in Fig. 6. The streamlines velocity for both expander stages was shown in Fig. 7 where the maximum flow velocity was about 245 m/s at nozzle exit of the first stage.

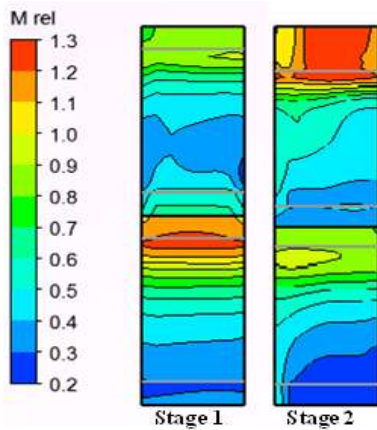


Fig. 4. Meridional distribution of relative Mach number distribution through stage 1 and stage 2 of the radial outflow expander.

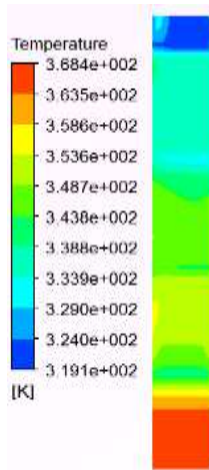


Fig. 5. Meridional temperature distribution through stage 1 and stage 2 of the radial outflow expander.

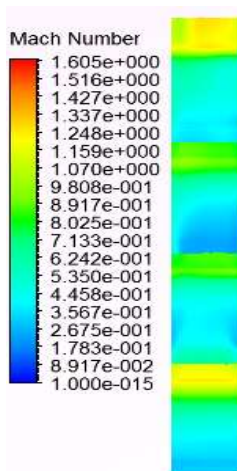


Fig. 6. Meridional Mach number distribution through stage 1 and stage 2 of the radial outflow expander.

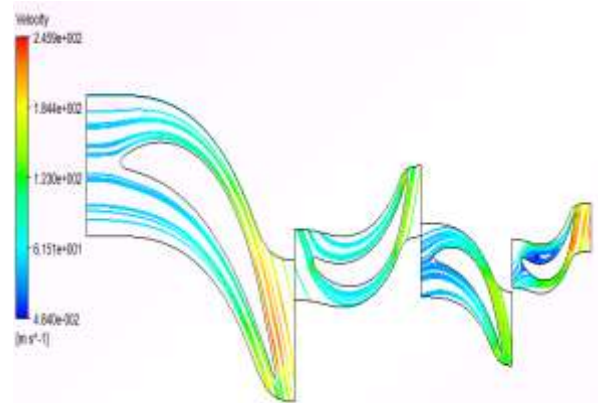


Fig. 7. Streamlines velocity through stage 1 and stage 2.

Fig. 8 demonstrates the variation of the expander efficiency and output power with various expansion ratios at the design conditions. This figure illustrates that the expander efficiency increases with increasing the expansion ratio until reaches peak value at the design point while the power output increases with the expansion ratio due to the increasing of the specific work done by the expander.

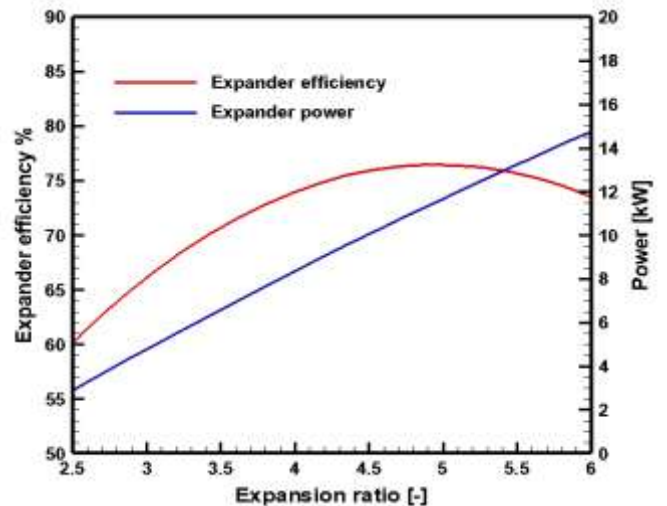


Fig. 8. Effect of expansion ratio on expander efficiency and power.

Based on thermodynamic analysis of the organic Rankine cycle (ORC), thermal efficiency of ORC system can be obtained according to the following equation:

$$\eta_{th} = \frac{\text{net power output}}{\text{thermal energy added}} \quad (10)$$

where  $\eta_{th}$  is the thermal efficiency of the ORC system.

The exergy efficiency of the ORC system is determined using the following equation:

$$\eta_{exs} = \frac{\text{net power output}}{Q_{add} \left[ \frac{(T_{in} - T_{atm} - T_{atm} \cdot \ln \frac{T_{in}}{T_{atm}})}{T_{in} - T_{atm}} \right]} \quad (11)$$

where  $\eta_{th}$ ,  $Q_{add}$ ,  $T_{in}$ ,  $T_{atm}$ , are the exergy efficiency, thermal energy added, temperature of working fluid at the expander inlet, and the atmospheric temperature respectively.

It can be found from Fig. 9 that thermal efficiency increases with increasing the inlet temperature of the working fluid at the expander inlet due to the increase power output with the increase of the temperature at expander inlet. While, the exergy efficiency decreases with increase the temperature of the working fluid R245fa.

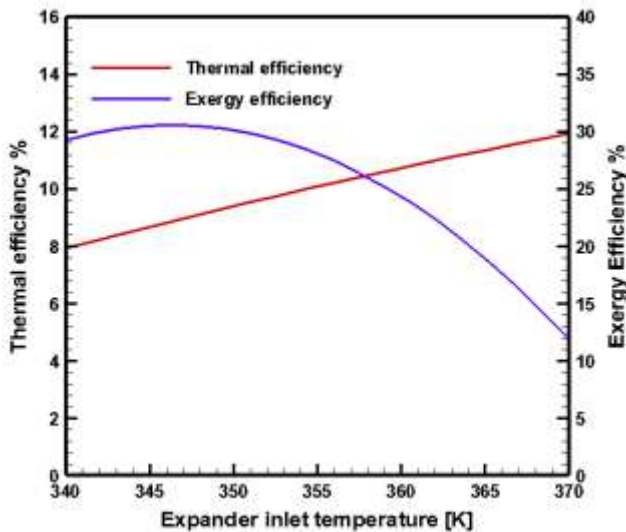


Fig. 9. Effect of expander inlet temperature on thermal efficiency and exergy efficiency.

### VI. CONCLUSION

In this research, the preliminary design and three dimensional simulations based on the computational fluid dynamics using CFX software were developed in order to study the performance of the radial outflow expander and organic Rankine cycle (ORC) system. Two stages configuration of the radial outflow expander was considered with working fluid R245fa with operating conditions in terms of 370 K and expansion ratio around 5.0 and rotational speed of 22000 rpm. Preliminary design was carried out using zTurbo while the three dimensional simulation was conducted using CFX software to predict the flow characteristic and aerodynamic performance. The results obtained from CFD simulations showed that the expander output power was around 15 kW and the expander efficiency was about 76%. Moreover, the Mach number showed that the flow was supersonic with Mach number of 1.6. According to the current study, the two stage of radial outflow expander is suitable for low output power applications.

### REFERENCES

[1] G. Persico, M. Pini, V. Dossena, and P. Gaetani, "Aerodynamic design and analysis of centrifugal turbine cascades," *ASME Turbo Expo 2013*:

*Turbine Technical Conference and Exposition*, American Society of Mechanical Engineers, pp. V06CT40A019-31, 2013.

[2] M. Pini, G. Persico, E. Casati, and V. Dossena, "Preliminary design of a centrifugal turbine for organic rankine cycle applications," *Journal of Engineering for Gas Turbines and Power*, vol. 135, p. 042312, 2013.

[3] E. Casati, S. Vitale, M. Pini, G. Persico, and P. Colonna, "Centrifugal turbines for mini-organic Rankine cycle power systems," *Journal of Engineering for Gas Turbines and Power*, vol. 136, p. 122607, 2014.

[4] A. M. Al Jubori, R. Al-Dadah, and S. Mahmoud, "Performance enhancement of a small-scale organic Rankine cycle radial-inflow turbine through multi-objective optimization algorithm," *Energy*, vol. 131, pp. 297-311, 2017.

[5] A. M. Al Jubori, R. Al-Dadah, and S. Mahmoud, "New performance maps for selecting suitable small-scale turbine configuration for low-power organic Rankine cycle applications," *Journal of Cleaner Production*, vol. 161, pp. 931-946, 2017.

[6] A. M. Al Jubori, R. Al-Dadah, and S. Mahmoud, "An innovative small-scale two-stage axial turbine for low-temperature organic Rankine cycle," *Energy Conversion and Management*, vol. 144, pp. 18-33, 2017.

[7] J. Hoffren, T. Talonpoika, J. Larjola, and T. Siikonen, "Numerical simulation of real-gas flow in a supersonic turbine nozzle ring," *Journal of Engineering for Gas Turbines and Power*, vol. 124, pp. 395-403, 2002.

[8] P. M. Congedo, C. Corre, and P. Cinnella, "Numerical investigation of dense-gas effects in turbomachinery," *Computers & Fluids*, vol. 49, pp. 290-301, 2011.

[9] G. Pei, J. Li, Y. Li, D. Wang, and J. Ji, "Construction and dynamic test of a small-scale organic rankine cycle," *Energy*, vol. 36, pp. 3215-3223, 2011.

[10] W. Pu, C. Yue, D. Han, W. He, X. Liu, Q. Zhang, et al., "Experimental study on Organic Rankine cycle for low grade thermal energy recovery," *Applied Thermal Engineering*, vol. 94, pp. 221-227, 2016.

[11] P. Colonna, J. Harinck, S. Rebay, and A. Guardone, "Real-gas effects in organic Rankine cycle turbine nozzles," *Journal of Propulsion and Power*, vol. 24, pp. 282-294, 2008.

[12] S. Quoilin, M. Van Den Broek, S. Declaye, P. Dewallef, and V. Lemort, "Techno-economic survey of Organic Rankine Cycle (ORC) systems," *Renewable and Sustainable Energy Reviews*, vol. 22, pp. 168-186, 2013.

[13] G. Manente, A. Toffolo, A. Lazzaretto, and M. Paci, "An Organic Rankine Cycle off-design model for the search of the optimal control strategy," *Energy*, vol. 58, pp. 97-106, 2013.

[14] W. Pu, C. Yue, D. Han, W. He, X. Liu, Q. Zhang, et al., "Experimental study on Organic Rankine cycle for low grade thermal energy recovery," *Applied Thermal Engineering*, vol. 94, pp. 221-227, 2016.

[15] M. K. Al-Ghezi, "Heat accumulation system for solar power station with parabolic trough solar collector," *Renewable Energy*, vol. 119, pp. 51122-51125, 2018.

[16] H.-Y. Wu and K.-L. Pan, "Optimum design and simulation of a radial-inflow turbine for geothermal power generation," *Applied Thermal Engineering*, vol. 130, pp. 1299-1309, 2018.

[17] R. Zhao, W. Li, W. Zhuge, Y. Zhang, Y. Yin, and Y. Wu, "Characterization of two-stage turbine system under steady and pulsating flow conditions," *Energy*, vol. 148, pp. 407-423, 2018.

[18] E. Casati, S. Vitale, M. Pini, G. Persico, and P. Colonna, "Centrifugal turbines for mini-organic Rankine cycle power systems," *Journal of Engineering for Gas Turbines and Power*, vol. 136, p. 122607, 2014.

[19] A. M. Al Jubori, R. K. Al-Dadah, S. Mahmoud, and A. Daabo, "Modelling and parametric analysis of small-scale axial and radial-outflow turbines for Organic Rankine Cycle applications," *Applied Energy*, vol. 190, pp. 981-996, 2017.